Nuclear Instruments and Methods in Physics Research A304 (1991) 679-682
North-Holland



# The semiconductor Cherenkov laser

NOTICE: THIS MATERIAL MAY BE
PROTECTED BY COPYRIGHT LAW
TITLE 17 U. S. CODE)

E.E. Fisch and J.E. Walsh

*Department of Physics and Astronomy, Dartmouth College, Hanover, NH 03755, USA*

A.K. Henning

*Thayer School of Engineering, Dartmouth College, Hanover, NH 03755, USA*

M.F. Kimmitt

*Department of Physics, University of Essex, Colchester, Essex, England, UK*

The semiconductor Cherenkov laser (SCL) is introduced. It is a low-voltage, tunable, far-infrared source of coherent radiation. The SCL exploits the interaction of a relativistic electron beam in close proximity to a semiconductor film. A related device is the Cherenkov free electron laser whose associated theory may be applied to the new device. General expressions for tuning and gain are considered in conjunction with electron beam, optical and material constraints to establish the operating characteristics.

## 1. Introduction

The semiconductor Cherenkov laser (SCL) is a novel low-voltage, tunable far-infrared (FIR) source of coherent radiation. A related device is the Cherenkov free electron laser (CFEL) whose associated theory can be applied to the new device. The SCL exploits the interaction of a relativistic electron beam in close proximity to a dielectric material. When electrons have a phase velocity greater than the speed of light in the medium, they emit spontaneous Cherenkov radiation. If the beam is slightly faster than the slow wave, electrons will bunch in the retarding phase and give energy to the mode. This radiation is guided by the slow-wave structure, and hence is confined to discrete waveguide modes. When the gain of the mode is sufficient to overcome resonator losses, coherent, high-power, tunable radiation can be extracted. Such a compact, powerful radiation source does not currently exist, and would have numerous applications in communications, medicine and spectroscopy. The advantages of the SCL over the traditional low-index CFELS are that: a lower voltage is required to obtain lasing at a given wavelength, charge buildup on the film surface is eliminated by the semiconductor's dc conductivity, and material/fabrication techniques for integrated circuits have advanced beyond any potential SCL resonator requirements. In order to be more specific about the device, a brief theory section is included. Si, GaAs, and Ge are used for numerical calculations because they are readily available, promising candidates for the SCL resonator material.

## 2. CFEL theory

The planar resonator is shown in fig. 1 with a sketch of the axial electric field amplitude. We define the direction perpendicular to the surface as $x$, and the direction of electron beam propagation as $z$. The beam must couple to the axial electric field ($E_z$), so only TM modes are considered. The specific resonator geometry and material determine the form of the electric and magnetic fields. Solving Maxwell's equations with the appropriate boundary conditions yields the dispersion relation

$$D(\omega d/c,\ kd,\ \text{geometry}) = 0, \qquad (1)$$

where $\omega$ is the angular frequency, $c$ is the speed of light and $k$ is the mode wavenumber. Eq. (1) is solved numerically to yield a characteristic relation between

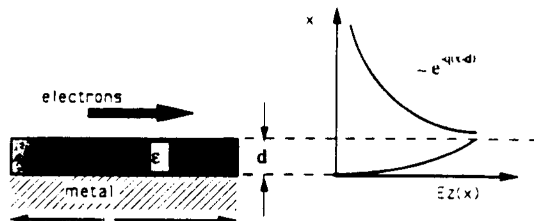


Fig. 1. The geometry of a planar semiconductor resonator of length $L$ and depth $d$ is shown. The electron beam passes a distance $\delta$ from the resonator surface. The $E_z$ field amplitude is sketched to illustrate the field/beam spatial overlap which is essential for FEL operation.

0168-9002/91/$03.50 © 1991 – Elsevier Science Publishers B.V. (North-Holland)

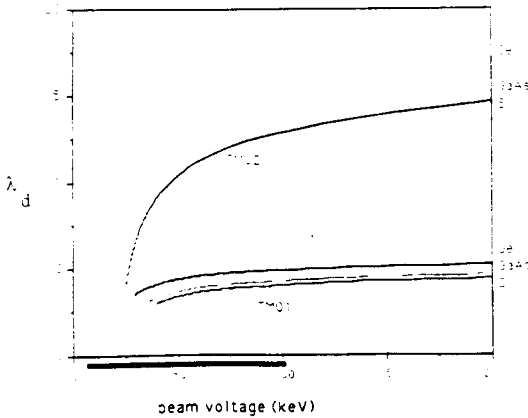


Fig. 2. The TM tuning curve for the two lowest order modes is plotted for Si, GaAs, and Ge whose FIR dielectric constants are 11.8, 12.9, and 16, respectively. The voltage range of interest is indicated on the axis by a heavy line.

$\omega d/c$ vs $kd$. The waveguide reduces the phase velocity of the wave from its free-space value ($\omega/ck = 1$). The effect is more pronounced for larger dielectric constants and thicker waveguides.

Since synchronism between the e.m. phase velocity and the electron beam's $\beta$ is necessary for bunching to occur, eq. (1) is, for practical purposes,

$$D(\omega d/c, \omega d/\beta c, \text{geometry}) = 0. \quad (2)$$

Cast in this form, the dispersion relation gives the operating wavelength ($\lambda = 2\pi c/\omega$) for a given kinetic energy. This is the tuning curve which is shown in fig. 2. At a given energy, the output wavelength decreases with smaller dielectric constants and/or thinner dielectric layers. A useful scaling law is apparent: $\lambda \sim d$.

The beam/electron interaction must provide gain at these established operating wavelengths. A derivation of the single-particle, one-dimensional gain is beyond the scope of this paper. The annotated expression itself should provide sufficient insight at this point. The gain per pass is defined as the rate of radiation amplitude growth times the time required for the electron beam to traverse the resonator. For an electron beam of width $\sigma_{bv}$ passing $\delta$ away from a resonator with mode width $w$, it is [7]

$$g = \frac{J_{b0}L^2}{mc^3/e}\,\frac{\sigma_{bv}}{w}\,\frac{L}{d} f_c g_0, \quad (3)$$

where $J_{b0}$ is the peak electron current density and $mc^3/e = 17$ kA. The geometric factors $L$ and $d$ are shown on fig. 1. $g_0$ depends only on the dispersion relation of the resonator and the single-particle gain line shape $F_R$. It is given by

$$g_0 = \frac{8\pi(\gamma^2 - \gamma_T^2)}{\beta^5\gamma^7\left(kd^{-1} + \gamma^{-1} + \epsilon(\gamma)^{-3}\right)} F_R(\kappa L), \quad (4)$$

where the relativistic factor evaluated at the Cherenkov threshold, $\beta = \epsilon^{-1/2}$, is

$$\gamma_T^2 = \frac{\epsilon}{\epsilon - 1}. \quad (5)$$

The familiar single-particle gain line shape function is

$$F_R(\kappa L) = \frac{2(1 - \cos \kappa L) - \kappa L \sin \kappa L}{(\kappa L)^3}, \quad (6)$$

where the relative phase shift between the electron velocity and the mode's phase velocity is

$$\kappa L = \left(k - \frac{\omega}{c\beta_0}\right) L. \quad (7)$$

The spatial overlap for an evanescent mode and an electron beam with height $\sigma_{bv}$ is evaluated via the coupling factor,

$$f_c = \exp\left(\frac{-4\pi\delta}{\lambda\beta\gamma}\right)\left[1 - \exp\left(\frac{4\pi\sigma_{bv}}{\lambda\beta\gamma}\right)\right] = e^{-\mu_\delta}(1 - e^{-\mu_b}). \quad (8)$$

For practical beam dimensions, the $\mu_\delta$ term dominates. The presence of a gap between the beam and semiconductor dramatically decreases the gain at low energies. Thus, the gain peak is shifted to slightly higher energies.

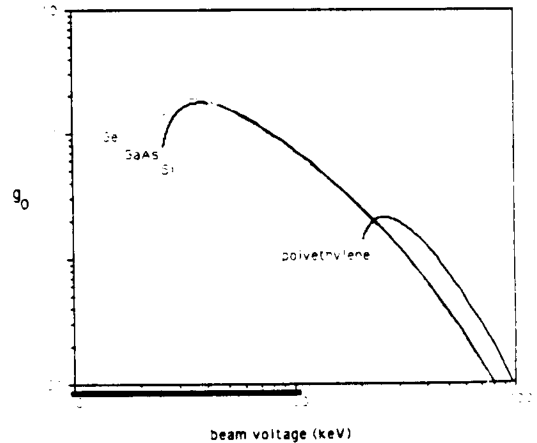


Fig. 3. The gain parameter $g_0$ is plotted for the first TM branch of Si, GaAs, and Ge. Polyethylene is included for comparison because is has been used in a higher voltage experiments. Here $\delta = 0$: including a finite gap would reduce the peak value and shift it to slightly higher energies. Again, the relevant voltage range is indicated with a heavy line on axis.

Calculations indicate that $\delta/d \approx 0.2$ is tolerable, though much better alignment can be achieved experimentally.

All functional dependencies in the gain are incorporated in $g_0$, eq. (4); it is this function that is plotted in fig. 3. Electrons whose phase allows maximum gain dominate the process, so we evaluate $g_0$ at the peak value of the single-particle line shape: $F_R(\kappa L = 2.34) = -0.135$. The semiconductors of interest (Si, Ge and GaAs) have an optimum gain at voltages of about 20–100 keV.

## 3. Semiconductor resonator considerations

The first concern is that the new material allows beam/optical mode spatial overlap. The longitudinal electric field has a simple exponential decay from the semiconductor surface into the vacuum, $E_z(x) = E_z e^{-qx}$, where $q^2 = k^2 - (\omega/c)^2$. The proportion of field in the vacuum and the field's evanescent length are easily calculated from the dispersion relation. Both were entirely acceptable for semiconductors in the voltage range of interest.

Losses must also be considered. The mode/beam interaction causes growth which must be sufficient to overcome the losses associated with propagation in the guide. For a dielectric waveguide of length $L$ with material losses $\alpha_m$ and end mirrors characterized by reflectivities $r_1$ and $r_2$, the losses are

$$\alpha_{\text{thresh}} = \frac{1}{2}\left(\alpha_m - \frac{1}{L}\ln(r_1 r_2)\right). \tag{9}$$

The factor 1/2 converts the amplitude-based derivation to the more familiar power loss form.

One way of decreasing resonator losses is to increase the mirror reflectivities, $r$. Only integral mirrors are treated because they eliminate losses associated with coupling out of the guide. They also offer the advantage of mechanical integrity. The simplest Fabry–Perot cavity is formed by cleaving and polishing the ends of the dielectric resonator. Typical $r$ values are about 30–40% for Si, GaAs and Ge. If an increased $r$ is desired, metal can be evaporated onto the end faces. A 200 nm layer of Al should provide near 100% reflection over the entire range of interest. Thickening the guiding layer at the resonator ends should confine the mode for more complete reflection.

Another way to reduce resonator losses is to minimize material losses, $\alpha_m$. In the FIR radiation and scattering losses are minimal, but we need to consider absorption. Semiconductor absorption is dominated by interband absorption. The threshold wavelength for this is $\lambda_g$ [μm] = $1.24/E_g$ [eV] where $E_g$ is the energy gap. This gap wavelength separates the absorption into two regions. The first corresponds to $\lambda < \lambda_g$ where intrinsic carriers are excited across the bandgap. This is a region of strong absorption which is avoided by a judicious choice of material. The second, $\lambda > \lambda_g$, is characterized by free-carrier absorption, lattice absorption, intraband absorption, and defect or dopant absorption. For relatively high resistivity materials in the FIR, free-carrier absorption dominates [8].

The Classical Drude theory expression for free-carrier absorption is

$$\alpha_{fc} = \frac{Nq^2\lambda^2}{8\pi^2 m^* nc^3\tau}, \tag{10}$$

where $N$ is the free-carrier concentration, $\lambda$ is the lasing wavelength, $m^*$ is the free-carrier effective mass in the semiconductor, $n$ is its index of refraction, and $\tau$ is the scattering lifetime. The Drude model is most applicable to metals, but it provides a first order indication of the absorption behavior. Namely, it is less significant at low temperatures, short wavelengths, and low carrier concentrations (high resistivities). The exponent of $\lambda$ actually varies between 1.5 and 2.5, depending upon whether acoustic or optical phonon modes are excited. Absorption due to ionized impurities goes as $\lambda^{3.5}$, but are negligible in semiconductors with resistivities above 40 Ω cm [8].

Finally, the resonator geometry must be considered. Introducing a trough-like curvature in the transverse ($y$) direction would improve the confinement of the optical mode. Propagation losses could be reduced by introducing a "buffer" layer of material with $\epsilon$ less that the semiconductor $\epsilon$. Despite the improvement in optical beam properties, these modifications have little effect on the dispersion relation. Hence, the theory which has been presented generally applies. The one exception is the tight radius through, and even this case does not deviate substantially from the planar structure. The

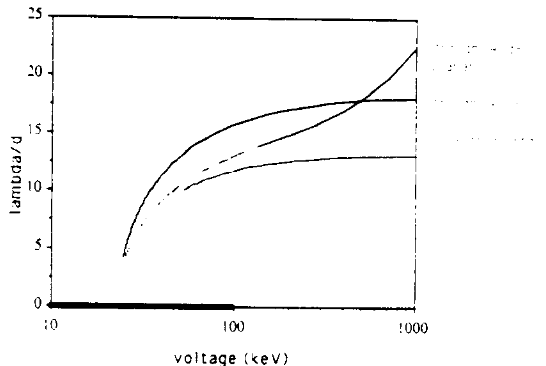


Fig. 4. The tuning curves for various geometries of a Si resonator are shown. In the relevant voltage range there is no significant shift of the curves with the possible exception of an extremely tight radius trough. Given the typical semiconductor depths $d$ for FIR operation, such a resonator would not be practical anyway.

tuning curve for various geometries shown in fig. 4 substantiates this.

## 4. A SCL design

The theory is applied to establish the operating parameters for a practical SCL device. A thin Si film on a metal substrate is chosen as the resonator. Rather than attempting to quantify losses, we assume that a gain of 1 will be obtained. This value is conservative, but ensures that threshold will be obtained for any reasonable resonator. For mid-FIR operation on the fundamental TM mode at voltages in the 50–100 keV range, a 50 μm thick film is implicated by the tuning curve of fig. 2. It is assumed that the waveguide mode width can be approximated by the Gaussian waist, ($w = \sqrt{L\lambda/2\pi}$). Table 1 summarizes the design calculations. The results indicate that operation of a thin-film Si resonator SCL at Dartmouth is well within theoretical constraints.

Table 1
Calculations for a Si film with $d = 50$ μm

| Parameter | Energy [keV] | | |
|---|---|---|---|
| | 30 | 50 | 100 |
| $\gamma = (511/\text{voltage [keV]}) + 1$ | 1.06 | 1.10 | 1.20 |
| $\beta = (1 - 1/\gamma^2)^{1/2}$ | 0.33 | 0.42 | 0.60 |
| $\lambda$ [μm] from tuning | 350 | 500 | 650 |
| $L$ [cm] for $L/\lambda = 100$ | 3.5 | 5.0 | 6.5 |
| $\delta$ [μm] for $\mu_\delta = 1$ | 18 | 29 | 42 |
| $\sigma_{bx}$ [μm] for $\mu_b = 4$ | 74 | 120 | 170 |
| $g_0$ from gain curve | 0.7 | 1.0 | 1.5 |
| $\sigma_{by}$ [μm] ($= \sigma_{bx}$) | 74 | 120 | 170 |
| $J_b(g = 1)$ [A/cm$^2$] | 148 | 31 | 9 |

## 5. Conclusions

The impetus for this work was to develop a low-voltage FIR laser source. Calculations show that such a device is easily realized with current technology. Introducing the semiconductor resonator has a number of advantages beyond reducing the Cherenkov threshold. There is improved gain at the low voltages. Finite dc resistivity should eliminate the charging which has been problematic in earlier < 200 keV experiments. Material availability and fabrication techniques are in excess of any potential resonator requirements. Finally, intrinsic semiconducting properties accommodate a host of potential improvements such as a variable-depth guiding layer, tunable dielectric constant, remote modulation and miniaturization.

## References

[1] J. Walsh, T. Marshall and S. Schlesinger, Phys. Fluids 20 (1977) 709.
[2] S. Von Laven, J. Walsh, J. Branscum, J. Golub and R. Layman, Appl. Phys. Lett. 41(5) (1982) 402.
[3] E. Garate, J. Walsh, S. Moustaizis, J.-M. Buzzi, C. Rouille, H. Lamain and B. Johnson, Appl. Phys. Lett. 48 (1986) 1326.
[4] E. Garate, R. Cooke, P. Heim, R. Layman and J. Walsh, J. Appl. Phys. 58 (1985) 627.
[5] E. Garate, J. Walsh, C. Shaughnessy and S. Moustaizis, Nucl. Instr. and Meth. A259 (1987) 125.
[6] J. Walsh, personal communication, May 1990.
[7] E. Fisch, A. Henning and J. Walsh, A Cherenkov microlaser, IEEE J. Quantum Electron., to be published.
[8] J.I. Pankove, Optical Processes in Semiconductors (Dover, New York, 1971), p. 75.